

SYNCHROTRON RADIATION ANALYSIS OF THE SUPERKEKB POSITRON STORAGE RING

J.A. Crittenden and D.C. Sagan
CLASSE*, Cornell University, Ithaca, NY 14850, USA
T. Ishibashi and Y. Suetsugu

High Energy Accelerator Research Organization (KEK), 1-1 Oho, Tsukuba, Ibaraki 305-0801, Japan

Abstract

We report on modeling results for synchrotron radiation absorption in the SuperKEKB positron storage ring vacuum chamber including the effects of photon scattering on the interior walls. A detailed model of the geometry of the inner vacuum chamber profile has been developed and used as input to a photon tracking code. Particular emphasis is placed on the photon absorption rates in the electron-positron interaction region.

INTRODUCTION

The SuperKEKB e^+e^- collider will provide high-precision measurements of the production and decay of bound states of B quarks in the interactions of 4-GeV positrons with 7 GeV electrons. Commissioning is scheduled to begin in 2016. The design of the vacuum system [1] incorporates a variety of countermeasures to limit electron cloud buildup in the positron ring. The Cornell Electron Storage Ring Test Accelerator (CESR-TA) program [2], in operation since 2008, has provided a wealth of information on the efficacy of such mitigation techniques via extensive measurements and model development which has also been used in the design of the International Linear Collider positron damping ring. [3, 4]. Here we report on results from a detailed modeling study of synchrotron radiation photon scattering and absorption on the interior surfaces of the vacuum chamber in the positron ring. In general, the effect of photon scattering on the walls of the vacuum chamber both adds and subtracts to the photon absorption rate (and therefore photoelectron production) at any point in the ring. However, such calculations can result in significant incident photon rates in regions where no synchrotron radiation strikes the wall directly.

VACUUM CHAMBER MODEL

Standard beam pipes in the positron storage ring have a circular beam channel and two rectangular antechambers on either side, as shown in Fig. 1. Synchrotron radiation photons irradiate the outer wall of the antechamber on the outside of the ring. The diameter of the beam channel and the half width at the horizontal axis are 90 mm and 110 mm, respectively. Strip-type non-evaporable getters (NEG) pumps are installed in the antechamber on the inside

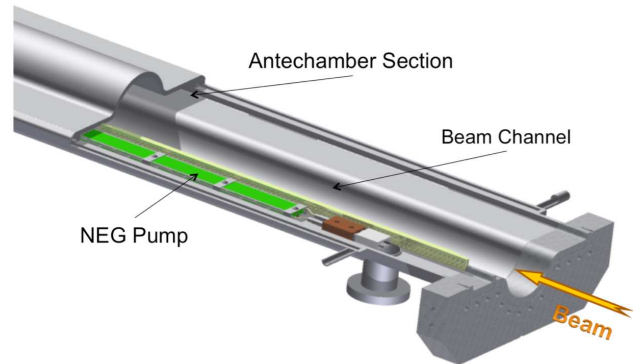


Figure 1: Schematic drawing of a beam pipe in arc sections of the positron storage ring.

of the ring. The pump channel is connected to the beam channel through a screen. A cross section of the standard beam pipe in the vacuum chamber model for the present calculations is shown in Fig. 2. The screens for the NEG pumps are defined as photon-absorbing walls in the model. In the wiggler sections, the photons strike both sides of the beam pipe, so both antechambers are used as channels for photon absorption. The rear walls of the antechambers are roughened to reduce scattering [1]; here we assume them to be totally absorptive. Circular beam pipes have been adopted in the interaction region (IR). The diameters vary in a staircase pattern from 80 mm at the entrance of the final focusing magnets (QCs) to 21 mm at the interaction point (IP). The beam pipes in the QCs on one side of the IP are

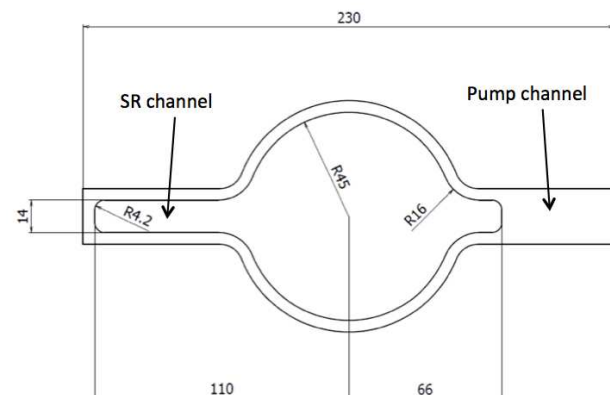


Figure 2: Cross section of the vacuum chamber model in the arc sections.

* Work supported by the US National Science Foundation contracts PHY-0734867, PHY-1002467, the U.S. Department of Energy contract DE-FC02-08ER41538 and the Japan/US Cooperation Program

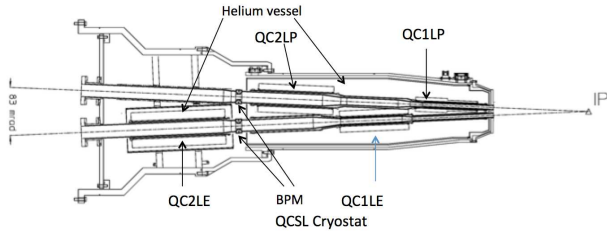


Figure 3: Schematic view from above of the beam pipes in the cryostat on one side of the IP. The positron beam exits on the left in the upper of the two pipes shown.

shown in Fig. 3. The beam pipes nearest the IP are tapered from 40 mm to 21 mm diameter in order to cut off the photons to the Belle-II detector. The beam pipes also have ridge structures on the inner surface to diffuse the photons. These structures are not included in the model described here.

SYNCHROTRON RADIATION PATTERN

Figure 4 shows a calculation of the synchrotron radiation pattern on the outside wall of the the 4-GeV positron ring, ignoring the effects of photon reflections. It comprises an analytic calculation of the synchrotron radiation rate from bending radii of the dipole magnets only and uses the distance of the wall from the beam in the horizontal midplane only. The linear density, per positron, of incident photons is averaged over 1-m intervals. The rate is less than 2 photons/m/e+ in the arcs, with hot spots reaching 10 photons/m/e+ downstream of the damping wiggler sections. No photons are directly incident on the outer wall within 10 m of the interaction point.

PHOTON TRACKING CODE SYNRAD3D

Analysis of the the CESR-TA measurements of electron-cloud-induced coherent tune shifts motivated the development of the Monte Carlo-based photon scattering and tracking code Synrad3D [5], since the important contribution of electron cloud buildup in dipole magnets depends directly on photons striking the top and bottom of the beam pipe near the vertical plane containing the beam [6]. The code

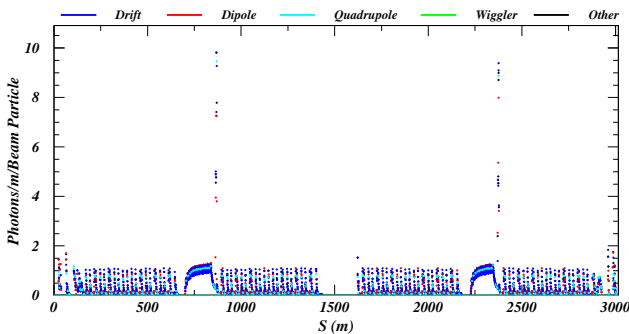


Figure 4: Analytic calculation of the synchrotron radiation pattern directly incident on the outside wall of the 4-GeV positron ring. The lattice element type in which the photons strike the wall is color-coded as shown.

employs tabulated information for X-ray specular and diffuse scattering from the LBNL database [7]. It implements a calculation of diffuse scattering probability based on electromagnetic theory (see, for example, Refs. [8] and [9]) with RMS roughness σ_r and transverse autocorrelation length T_{corr} as input parameters. For these simulations, values typical of technical vacuum chamber surfaces were used: $\sigma_r = 100$ nm and $T_{\text{corr}} = 5000$ nm. These values were applied in the successful modeling of CESR-TA coherent tune shifts measurements [10]. For the results discussed below, photons with energies less than 4 eV were not included in the absorption rates.

DISTRIBUTION OF ABSORBED PHOTONS

Figure 5 shows characteristics of photons absorbed around the entire ring, including the effects of photon scattering. Figure 5 a) shows the transverse absorption coordinates integrated over the ring circumference, exhibiting the variety of beam pipe cross sections in the vacuum system design, including the antechambers and the 21-mm-diameter pipe in the IR. Figure 5 b) shows the linear density, per positron, of absorbed photons. This density increases by about 50% to 2 photons/m/e+ in the wiggler regions when

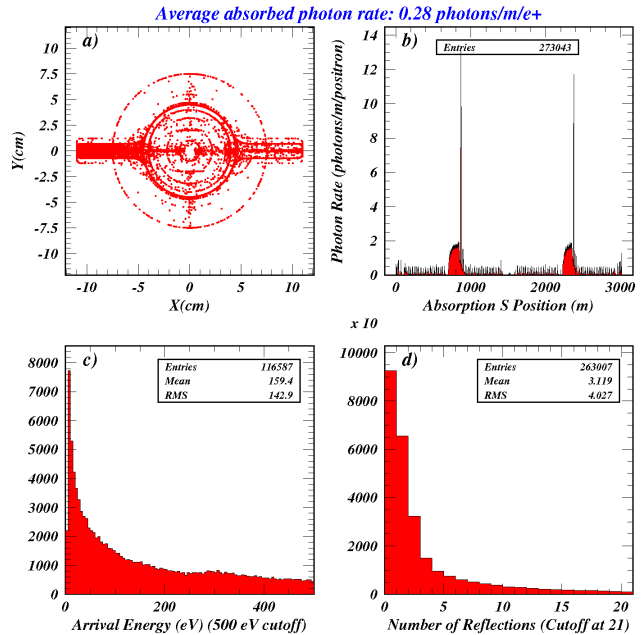


Figure 5: Distributions of absorbed photons around the ring including the effects of photon scattering. a) Scatter plot of vertical versus horizontal photon absorption coordinates integrated over the ring circumference, exhibiting the variety of transverse vacuum chamber profiles, including the antechambers. b) Distribution of absorbed photon locations in the arc coordinate S of the positron orbit, ranging up to 3016.31 m. c) Distribution of absorbed photon energies below 500 eV. d) Number of wall reflections undergone by the photons prior to absorption.

photon scattering is taken into account, and increases to 12-14 photons/m/e+ in the two hot spots downstream of the wigglers. For the design beam current of 3.6 A, 1 photon/m/e+ corresponds to a rate of 2.3×10^{19} photons/m/s. The average energy of absorbed photons is about 160 eV, as shown in Figure 5 c). Figure 5 d) shows that about 90k of the 263k modeled photons are absorbed without previously having scattered. The average number of reflections around the ring prior to absorption is 3.1.

The rate of photons absorbed in the IR is of special concern for electron cloud buildup in regions where the beta functions are large [11]. Figure 6 shows the characteristics of photons absorbed within 10 m of the IP. The 5-cm-diameter mask near the IP prevents photons from hitting the wall in the downstream region from 1 m to 7 m from the IP, but there is a small rate of photons absorbed in the QC1LP magnet ($0.76 < S < 1.1$ m).

The design of the final focus magnet system includes 8 superconducting magnets located within 3 m of the e+e- interaction point [12, 13]. Here we report on modeling results for the example of the magnet closest to the IP in the positron ring on the upstream side, the 334-mm-long QC1RP magnet, the center of which is located 935 mm from the IP. The field gradient in this quadrupole magnet is 68.7 T/m. The analytic calculation of the synchrotron radiation incident on the beam pipe wall, and the photon scattering model with scattering turned off, each find a low rate of incident pho-

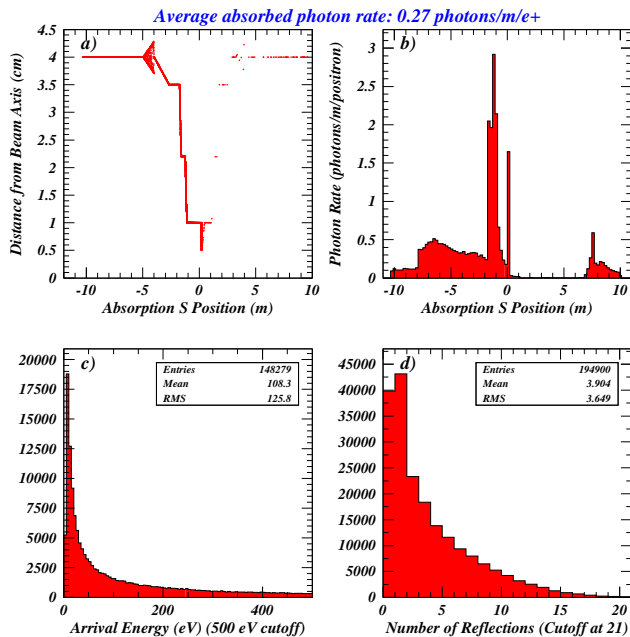


Figure 6: Distributions of photons absorbed within 10 m of the IP. a) Scatter plot of the distance of the absorbed photons from the beam axis, showing the radius transitions in the vacuum chamber. b) Distribution of absorbed photon locations in the arc coordinate S of the positron orbit, ranging from -10 to 10 m. c) Distribution of absorbed photon energies below 500 eV. d) Number of wall reflections undergone by the photons prior to absorption.

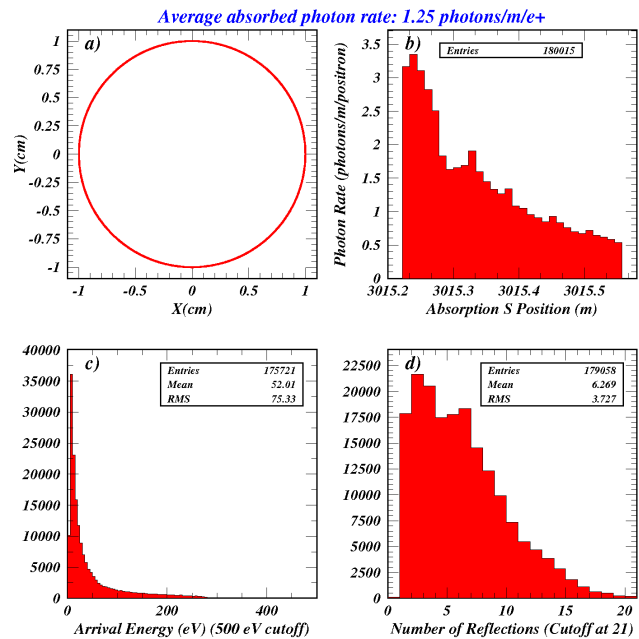


Figure 7: Distributions of absorbed photons in the final-focus quadrupole magnet QC1RP.

tons of about 0.04 photons/m/e+ originating in an anti-bend magnet 5 m upstream of QC1RP. With photon scattering enabled in the model, the absorbed photon density increases by a factor of nearly 30 to 1.25 photons/m/e+, comparable to the maximum rates reached in the arcs. Figure 7 shows the distributions for photons absorbed in the walls. No photons are absorbed which have not previously scattered at least once, i.e. the directly incident photons strike the wall at such shallow incident angle and low energy that the absorption rate is negligible. A substantial fraction of the photons are absorbed in regions where the photoelectrons produced can be trapped in the quadrupole field. The average energy of all absorbed photons is about 50 eV.

SUMMARY

We have applied the X-ray photon tracking and scattering/absorption code Synrad3D to the positron ring of the SuperKEKB e+e- collider. When the effects of photon scattering are thus taken into account, the rate of absorbed photons is comparable to the incident rate of photons without scattering effects at the level of about 50%. However, the calculated rate of absorbed photons is dramatically higher in regions where no light hits the walls directly, such as near the IP. We find that the predicted rate for photon absorption within 10 m of the IP is comparable to the ring-averaged rate. In the particular case of the upstream final-focus quadrupole nearest the IP, the modeled rate is found to be 1.25 photons/m/e+, which is about half the rate in the wiggler regions and comparable to the highest rates reached in the arcs of the ring. An initial study of the consequences of such a rate of absorbed photons for electron cloud buildup in the final-focus quadrupoles is contributed to these proceedings [14].

REFERENCES

- [1] Y. Suetsugu *et al.*, “Design and Construction of the SuperKEKB Vacuum System,” *J. Vac. Sci. Technol. A* **30**, 031602 (May 2012).
- [2] G. F. Dugan, M. A. Palmer & D. L. Rubin, “ILC Damping Rings R&D at CESR-TA,” in *ICFA Beam Dynamics Newsletter*, J. Urakawa, Ed., International Committee on Future Accelerators, No. 50, p. 11–33 (Dec. 2009).
- [3] J. A. Crittenden *et al.*, “Investigation into Electron Cloud Effects in the International Linear Collider Positron Damping Ring,” *Phys. Rev. ST Accel. Beams* **17**, 031002 (Mar. 2014).
- [4] M. T. F. Pivi *et al.*, “Recommendation for Mitigations of the Electron Cloud Instability in the ILC,” in *Proceedings of the 2011 International Particle Accelerator Conference, San Sebastián, Spain*, EPS-AG (2011), p. 1063–1065.
- [5] G. Dugan & D. Sagan, “SYNRAD3D Photon Propagation and Scattering Simulations,” in *Proceedings of ELOUD 2012: Joint INFN-CERN-EuCARD-AccNet Workshop on Electron-Cloud Effects, La Biodola, Elba, Italy*, R. Cimino, G. Rumolo & F. Zimmermann, Eds., CERN, Geneva, Switzerland (2013), CERN-2013-002, p. 117–129.
- [6] “The CESR Test Accelerator Electron Cloud Research Program: Phase I Report,” Tech. Rep. CLNS-12-2084, LEPP, Cornell University, Ithaca, NY (Jan. 2013).
- [7] B. L. Henke, E. M. Gullikson & J. C. Davis, “X-Ray Interactions: Photoabsorption, Scattering, Transmission, and Reflection at $E = 50\text{--}30,000$ eV, $Z = 1\text{--}92$,” *At. Data Nucl. Data Tables* **54**, p. 181–342 (Jul. 1993).
- [8] P. Beckmann & A. Spizzichino, *The Scattering of Electromagnetic Waves from Rough Surfaces*, Pergamon Press, New York (1963).
- [9] J. A. Ogilvy, *Theory of Wave Scattering from Random Rough Surfaces*, Hilger, Bristol (1993).
- [10] G. Dugan *et al.*, “Observations and Predictions at CesrTA, and Outlook for ILC,” in *Proceedings of ELOUD 2012: Joint INFN-CERN-EuCARD-AccNet Workshop on Electron-Cloud Effects, La Biodola, Elba, Italy*, R. Cimino, G. Rumolo & F. Zimmermann, Eds., CERN, Geneva, Switzerland (2013), CERN-2013-002, p. 31–41.
- [11] K. Ohmi & D. Zhou, “Study of Electron Cloud Effects in SuperKEKB,” in *IPAC2014: Proceedings of the 5th International Particle Accelerator Conference, Dresden, Germany*, C. Petit-Jean-Genaz *et al.*, Eds., JACoW, Geneva, Switzerland (2014), p. 1597–1599.
- [12] M. Tawada *et al.*, “Design Study of Final Focusing Superconducting Magnets for the SuperKEKB,” in *Proceedings of the 2011 International Particle Accelerator Conference, San Sebastián, Spain*, EPS-AG (2011), p. 2457–2459.
- [13] N. Ohuchi *et al.*, “Design of the Superconducting Magnet System for the SuperKEKB Interaction Region,” in *PAC 2013: Proceedings of the 2013 Particle Accelerator Conference, Pasadena, CA, USA*, T. Satogata, C. Petit-Jean-Genaz & V. Schaa, Eds., JACoW (2013), p. 843–845.
- [14] J. A. Crittenden, “Initial Modeling of Electron Cloud Buildup in the Final-focus Quadrupole Magnets of the SuperKEKB Collider,” in *IPAC2015: Proceedings of the 6th International Particle Accelerator Conference, Richmond, Virginia, USA*, C. Petit-Jean-Genaz *et al.*, Eds., JACoW, Geneva, Switzerland (2015).